IEEE Access
Multidisciplinary ⋮ Rapid Review ⋮ Open Access Journal

Received June 26, 2018, accepted July 31, 2018, date of publication August 10, 2018, date of current version September 7, 2018.

Digital Object Identifier 10.1109/ACCESS.2018.2864629

Nighttime Driving Safety Improvement via Image Enhancement for Driver Face Detection

JIANHAO SHEN[1], GUOFA LI[2,3], WEIQUAN YAN[2], WENJIN TAO[4], GANG XU[1], DONGFENG DIAO[5], AND PAUL GREEN[6,7]

[1]Shenzhen Key Laboratory of Urban Rail Transit, College of Mechatronics and Control Engineering, Shenzhen University, Shenzhen 518060, China
[2]College of Mechatronics and Control Engineering, Institute of Human Factors and Ergonomics, Shenzhen University, Shenzhen 518060, China
[3]State Key Laboratory of Automotive Safety and Energy, Department of Automotive Engineering, Tsinghua University, Beijing 100084, China
[4]Department of Mechanical and Aerospace Engineering, Missouri University of Science and Technology, Rolla, MO 65409, USA
[5]Guangdong Provincial Key Laboratory of Micro/Nano Optomechatronics Engineering, Institute of Nanosurface Science and Engineering, Shenzhen University, Shenzhen 518060, China
[6]University of Michigan Transportation Research Institute, Ann Arbor, MI 48109, USA
[7]Department of Industrial and Operations Engineering, University of Michigan, Ann Arbor, MI 48109, USA

Corresponding author: Guofa Li (guofali@szu.edu.cn)

This work was supported in part by the National Natural Science Foundation of China under Grant 51805332 and Grant 51577120, in part by the Science and Technology Development Foundation of Shenzhen Government under Grant JCYJ20140418182819128, in part by the Natural Science Foundation of SZU under Grant 2017033, and in part by the State Key Laboratory of Automotive Safety and Energy under Project KF1801.

ABSTRACT Insufficient illumination makes driver face detection at night challenging. This paper proposes an adaptive attenuation quantification retinex (AAQR) method to enhance the details of nighttime images. There are three phases in this method: attenuation restriction, attenuation prediction, and adaptive quantification. The performance of the proposed method was evaluated by employing a robust face detection method via sparse representation. The collected driver face images at night were categorized into three groups (up-down, left-right, and mixed) according to the illumination distribution in each image. Results have shown that the detection rates of the images enhanced by the proposed AAQR method were 82%, 84%, and 91% for the up-down, left-right, and mixed illumination groups, respectively. In comparison to other image enhancement methods, the detection rate of the AAQR method was 2%–36% greater. Furthermore, the mean computing time for a single 640 × 480 nighttime image using AAQR was less than most of the compared advanced methods. Thus, the AAQR method is recommended for applications in driver face detection tasks at night.

INDEX TERMS Advanced driver assistance systems, driver face detection, nighttime driving safety, image enhancement.

I. INTRODUCTION

Fatigue driving has been recognized as a significant cause of traffic accidents. More than 30% drivers in the U.S. drive with fatigue at least once a month [1]. In 2014, 846 people died because of fatigue while driving in the U.S., accounting for 2.6% of all fatalities [2]. In China, 537 people died because of fatigue driving on highways in 2010, accounting for 8.5% of all highway crashes. To detect fatigue, a number of indicators have been examined, including (1) vision-related indicators (e.g., eyelid movement, gaze movement, head movement and facial expression) [3]; (2) driving performance characteristics (e.g., entropy of the steering wheel angle) [5], [6]; and (3) physiological indicators (e.g., EEG) [7]–[9]. Among these efforts, vision-related indicators are the dominant approach [10], [11].

However, most of these efforts only focus on drivers' face detection in the daytime, ignoring nighttime driving where fatigue is common [12]–[14]. Specifically, in Queensland (Australia), fatigue-related crashes between 10 pm and 6 am accounted for 51.9% of all crashes, whereas during that same time period only 5.2% of all crashes were not fatigue related [15]. Therefore, for an automation system to return control to a driver, that system needs to know if the driver is able to takeover, which includes knowing if the driver is not too fatigued to do so. Prior to the fatigue detection, effective driver face detection at night is the primary problem that needs to be solved [3], [16].

Among the fewer attempts to detect driver faces in nighttime, near-infrared lighting systems are commonly employed to compensate the illumination [17], [18]. Based on the

images collected under near-infrared lighting situations, Histogram of Oriented Gradients (HOG) and Haar-like features have been commonly used to detected driver faces at night [21]. A face detection rate of 98% was reported when drivers were looking straight ahead at night [21]. When the clear face images are ready using near-infrared techniques, probabilistic models could be proposed to classify or to predict driver states (e.g., fatigue) using features extracted from drivers' head movement, facial expression and/or eye dimensions [19], [20]. The models could achieve promising capabilities in detection accuracy and real-time processing in different illumination conditions. Although these near-infrared illumination systems do not impact on driver's vision and work well in nighttime, their performance will drop dramatically due to the presence of external light sources which commonly exist in real traffic [13], [22], [23]. Also, The non-uniform and changing lighting distribution on a driver's face strongly restricts the effectiveness of the near-infrared systems [24]. Another limitation of the near-infrared system is that the color will be obviated in near-infrared images, and some useful information of the images will be thrown away.

Other attempts to detect driver faces in nighttime focus on illumination image enhancement. To achieve this goal, Retinex theory is commonly adopted to achieve color constancy and dynamic range compression by imitating human visual system [25]. The chromatic dominant of light and possible smooth shadows could lowered by using Retinex, thus the image details and edges were enhanced [26]. Based on the basic center/surround Retinex, various Retinex-based methods have been proposed to overcome its disadvantages, including Single Scale Retinex (SSR), Multi-Scale Retinex (MSR), Multi-Scale Retinex with Color Restoration (MSRCR), etc. [27]–[29]. They have proven to be useful in edge detection, image segmentation, and image analysis [28]. For a review of Retinex and the derived models, see [30].

Among the attempts using these methods, Rahman et al. tried to enhance an image using MSRCR before compression to figure out the relationship between image enhancement and compression [31]. Results showed that the image quality could be improved by applying MSRCR image enhancement before compression. Jiang *et al.* [32] proposed an improvement of MSRCR to eliminate the impact of outliers in the histogram of an image. Results showed an improvement in the contrast of an image with time-expensive computation to limit its real-time applications. Kuang *et al.* [33] adopted MSR to enhance nighttime images, and further extracted regions-of-interest for vehicle detection to find out a 93% detection rate at night. Wang *et al.* [34] proposed a Naturalness Preserved Enhancement algorithm (NPE) to enhance contrast while preserving naturalness of illumination. Fu *et al.* [35] proposed a Multi-deviation Fusion method (MF) to adjust the illumination by fusing multiple derivations of the initially estimated illumination map. A Simultaneous Reflection and Illumination Estimation (SRIE) algorithm was proposed in [36] to enhance images by manipulating the illumination with the estimated reflectance and illumination. Guo *et al.* [37] proposed a Low-light Image Enhancement Method (LIME) to exploit the structure of the illumination by developing structure-aware smoothing model to obtain the well-constructed illumination map. Dong *et al.* [38] proposed an optimized de-hazing based method (DONG) to enhance poor-lighting videos. Others studies like [39]–[43] also have enhanced the image quality a lot. See Table 1 for a comparative analysis of the above-mentioned methods. However, rarely do they examine the effectiveness of these improvements on driver face detection in nighttime driving. Also, they have not tested the robustness where the illumination is continually changing, a situation that commonly exists in real driving at night.

TABLE 1. A comparative analysis of the above-mentioned methods.

#	Publication year	Enhancement method	How the enhancement works
[32]	2015	MSRCR	Using multiple Gaussian filters with color restoration to separate reflectance and illumination
[34]	2013	NPE	Designing a bright-pass filter to estimate the illumination, and proposing a bi-log transformation to adjust the illumination
[35]	2016	MF	Adjusting the illumination by fusing multiple derivations of the initially estimated illumination map
[36]	2016	SRIE	Manipulating the illumination with the estimated reflectance and illumination
[37]	2017	LIME	Developing structure-aware smoothing model to exploit the structure of the illumination to refine the well-constructed illumination map
[38]	2011	DONG	Applying dark channel prior based image de-hazing algorithm to the inverted low lighting image

This paper proposes an illumination-robust image processing method to enhance driver face image details collected by visible light cameras under various illumination situations, especially in the environment with dynamically changing light. A face recognition method is employed to examine the effectiveness of the proposed method from the aspects of recognition accuracy and computing time.

The remainder of this paper is organized as follows: Section II describes the details of the proposed AAQR method for image enhancement. The employed face recognition method is also introduced in this section. Driver face images collection at night is described in Section III. The effectiveness of the proposed method is presented in Section IV. Section V describes the advantages of AAQR in comparison with other state-of-the-art methods under various illumination situations and discusses the future applications of the method for driver face detection. Section VI concludes this paper.

II. METHODS

A. ORIGINAL RETINEX MODEL

The Retinex theory can enhance details for images taken under complex lighting conditions. The most conventional Retinex model is processed in logarithm space because it is more straightforward and decreases complexity [25]. The original Retinex model is described as follows:

$$\begin{aligned} I(x,y) &= R^i(x,y) * L(x,y) \\ logR^i(x,y) &= logI(x,y) - logL(x,y) \end{aligned} \tag{1}$$

where $I(x,y)$ is the original image, $R^i(x,y)$ is a reflected image (Retinex image, $i \in \{R,G,B\}$) and $L(x,y)$ is a luminance image. As $L(x,y)$ cannot be obtained directly from the original image [25], it always can be approximated by convoluting the original image $I(x,y)$ with a Gaussian kernel function $F_n(x,y)$ [44], [45]. Therefore, $L(x,y)$ can be simplified as:

$$L(x,y) = F_n(x,y) * I(x,y) \tag{2}$$

According to (1) and (2), $R^i(x,y)$ can be obtained as follows:

$$R^i(x,y) = exp(I(x,y) - F_n(x,y) * I(x,y)) \tag{3}$$

$$F_n(x,y) = \lambda e^{-(x^2+y^2)/\sigma_n^2} \tag{4}$$

where σ_n is a Gaussian surround space constant and λ is a normalized factor which is determined to satisfy (5):

$$\iint F_n(x,y)dxdy = 1 \tag{5}$$

As reported in [46]–[48], $R^i(x,y)$ is strongly influenced by the value of the re-quantized pixel. Thus, a proper selection of quantization range is critical for image enhancement. A smaller quantization range decreases noises but may lose more image information. On the contrary, a larger quantization range retains image information but bring more noises. Therefore, how to select an appropriate quantization range is an important issue that is worth studying.

B. ADAPTIVE ATTENUATION QUANTIFICATION RETINEX (AAQR)

To enhance drivers' face image collected at night so that the face detection rate can be improved, this paper proposes a new illumination-robust image-processing method – AAQR. The AAQR belongs to the Retinex-based category as introduced above. The main idea of the AAQR is an adaptive strategy on the scaled distribution of the image information. The implementation of AAQR follows the three steps in Fig. 1: attenuation restriction, attenuation prediction, and adaptive quantification.

1) ATTENUATION RESTRICTION

In most digital images, the mean of pixels reflects the brightness level of the image, while the variance reflects the illumination stability. Hence, the brightness range of an image can be approximately computed by the mean and variance of the pixels. The more stable the image pixels are, the more concentrated the pixel value range is, and the larger the attenuated area is. A maximum attenuation coefficient is used to evaluate the attenuation range that can be applied to an image [49].

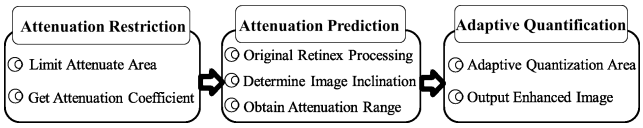

FIGURE 1. Flow of the proposed AAQR algorithm.

$$^ik_{lim} = log|\frac{^iI_{ave}}{^iI_{var}}| \tag{6}$$

where $^iI_{ave}$ is the mean of gray scale in each color channel, $^iI_{var}$ is the variance of gray scale in each color channel, and $^ik_{lim}$ is the maximum attenuation coefficient.

2) ATTENUATION PREDICTION

The Retinex image of the logarithmic domain $^iR_{log}(x,y)$ is computed as:

$$^iR_{log}(x,y) = logR^i(x,y) \tag{7}$$

As mentioned in (1), $^iR_{log}(x,y)$ is obtained by subtracting the low-pass filtered image from the original image in the logarithmic domain.

The distribution of the area information in each color channel should be computed respectively. In this paper, the area information of the $^iR_{log}(x,y)$ can be obtained through the median and mean of the $^iR_{log}(x,y)$ as:

$$\begin{aligned} ^iR_{log}^{med} &= \frac{max_{(x,y)\in\Omega}(^iR_{log}(x,y)) + min_{(x,y)\in\Omega}(^iR_{log}(x,y))}{2} \\ ^iR_{log}^{ave} &= \frac{1}{xy}\sum_{(x,y)\in\Omega} {}^iR_{log}(x,y) \end{aligned} \tag{8}$$

where $^iR_{log}^{med}$ and $^iR_{log}^{ave}$ are the median and mean of the $^iR_{log}(x,y)$, respectively. By comparing the size of $^iR_{log}^{med}$ and $^iR_{log}^{ave}$, the location of the image's principal information can be determined to be on the left or right side of $^iR_{log}^{med}$. This paper defines the left side of $^iR_{log}^{med}$ as the low area and the right side as the high area (See Fig. 2).

Based on the computed $^iR_{log}^{ave}$ and $^iR_{log}^{med}$, the square root of the maximum singular value of the high area and the low area are computed to describe the most important component of the image information in the two areas. Thus, the principal component coefficients of the high area $^ik_{high}$ and the low area $^ik_{low}$ are defined as:

$$\begin{aligned} ^ik_{low} &= ||^iR_{log}(x,y) - {}^iR_{log}^{med}(x,y) + {}^iR_{log}^{ave}(x,y)||_2 \\ ^ik_{high} &= ||^iR_{log}^{med}(x,y) - {}^iR_{log}(x,y) + {}^iR_{log}^{ave}(x,y)||_2 \end{aligned} \tag{9}$$

where $^iR_{log}^{med}(x,y)$ equals $^iR_{log}(x,y)$ when all the pixels are with gray scale of $^iR_{log}^{med}$, and $^iR_{log}^{ave}(x,y)$ equals $^iR_{log}(x,y)$

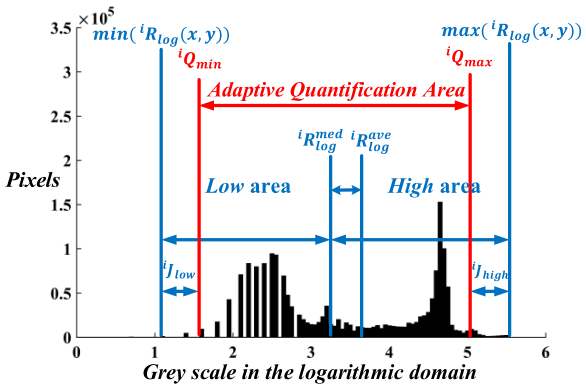

FIGURE 2. The area information of AAQR.

when all the pixels are with the gray scale of ${}^iR_{log}^{ave}$. The minimum and maximum boundaries of the adaptive quantification area can be obtained via the attenuation range ${}^iJ_{low}$ and ${}^iJ_{high}$:

$$\begin{cases} {}^iJ_{low} = \left| \frac{{}^ik_{low}}{{}^ik_{high}} \left({}^iR_{log}^{med} - {}^iR_{log}^{ave} \right) \right| \leq {}^ik_{lim} \\ {}^iJ_{high} = \left| \frac{{}^ik_{high}}{{}^ik_{low}} \left({}^iR_{log}^{med} - {}^iR_{log}^{ave} \right) \right| \leq {}^ik_{lim} \end{cases} \quad (10)$$
$$\begin{aligned} {}^iQ_{max} &= max({}^iR_{log}(x,y)) - {}^iJ_{high} \\ {}^iQ_{min} &= min({}^iR_{log}(x,y)) + {}^iJ_{low} \end{aligned}$$

where ${}^iQ_{max}$ and ${}^iQ_{min}$ are the maximum and minimum of the quantization area, respectively.

3) ADAPTIVE QUANTIFICATION

To avoid negative values in the quantization process, the pixels of attenuation area must be assigned new gray scales. The assignment for the pixels in the attenuation area is defined according to the following rules:

$$\begin{cases} if\ \overline{{}^iR_{log}} - {}^iQ_{min} < 0 \quad \overline{{}^iR_{log}} = {}^iQ_{min} \\ if\ \overline{{}^iR_{log}} - {}^iQ_{max} > 0 \quad \overline{{}^iR_{log}} = {}^iQ_{max} \end{cases}$$
$$\overline{{}^iR_{log}} = {}^iR_{log}(x_1, \quad y_1) x_1 \in x,\ y_1 \in y \quad (11)$$

where $\overline{{}^iR_{log}}$ denotes the pixel gray scale of ${}^iR_{log}(x,y)$.

Finally, the enhanced image $R^i(x,y)$ using AAQR is:

$$R^i(x,y) = \frac{{}^iR_{log}(x,y) - {}^iQ_{min}}{{}^iQ_{max} - {}^iQ_{min}} * 255 \quad (12)$$

The procedure of the proposed AAQR is outlined in Table 2.

TABLE 2. Outline of the proposed method.

Algorithm: AAQR

Input: An image with low illumination level.

Initialization: Constructing Gaussian kernel function using (4)

Compute

1. Estimate maximum attenuation coefficient ${}^ik_{lim}$ using (6);
2. Calculate ${}^iR_{log}^{med}$ and ${}^iR_{log}^{ave}$ using (8);
3. Get principal component coefficients from ${}^iR_{log}^{med}$ and ${}^iR_{log}^{ave}$ using (9);
4. Obtain attenuation range based on principal component coefficients ${}^ik_{low}$ and ${}^ik_{high}$ using (10);
5. Determine quantization area ${}^iQ_{max}$ and ${}^iQ_{min}$ using the attenuation range ${}^iJ_{low}$ and ${}^iJ_{high}$;
6. Re-quantified ${}^iR_{log}(x,y)$ according to quantization area using (11).

Output: Final enhanced image.

C. FACE DETECTION

In this paper, a face detection method is used to assess the performance of the proposed AAQR algorithm. The phases of the face detection method include face detection, face alignment and face validation. This method has been successfully applied in a face detection tool [50], [51].

1) FACE DETECTION

This paper extracts the HOGs features as proposed by [47]. Object's appearance and shape can be described by the gradient or directional density distribution. The amplitude and direction of the gradient at a single pixel are calculated as follows:

$$\begin{aligned} \mathrm{G}(x,y) &= \sqrt{G_x(x,y)^2 + G_y(x,y)^2} \\ \alpha(x,y) &= \tan^{-1} \frac{G_y(x,y)}{G_x(x,y)} \end{aligned} \quad (13)$$

where $G_x(x,y)$, $G_y(x,y)$ are the horizontal gradient and vertical gradient. $\mathrm{G}(x,y)$ and $\alpha(x,y)$ are the magnitude and orientation of the intensity gradient, respectively. Each pixel calculates a weighted vote for a histogram channel based on the orientation of the gradient elements centered around it.

2) FACE ALIGNMENT

Drivers may face a camera at angles. Thus, the collected images were re-aligned to improve the robustness. The employed face alignment function includes two phases: face landmark estimation and affine transformation.

- **Face landmark estimation**

An ensemble of regression trees was an effective algorithm in finding the critical characteristics by marking 68 features in a face image [53]. The features covered details of eyes, nose, mouth, shape of a face, etc. Taking shape estimation as an example, the image update function is defined as:

$$\hat{S}^{(t+1)} = \hat{S}^{(t)} + \mathrm{r}_t(I, \hat{S}^{(t)}) \quad (14)$$

where $\hat{S}^{(t)}$ is the current shape estimation, $\mathrm{r}_t(I, \hat{e}^{(t)})$ is the update vector derived from the input image I and the current shape estimation $\hat{S}^{(t)}$ in each iteration.

- **Affine transformation**

Affine transformation is a linear transformation from a 2D coordinate to another 2D coordinate while keeping the picture's straightness and parallelism. Using this transformation function, a side face can be transformed into a standard face, so that the processed image can be fed into a face

detection system. The transformation formula is defined as:

$$\begin{bmatrix} X' \\ Y' \\ 1 \end{bmatrix} = \begin{bmatrix} m_{00} & m_{01} & m_{02} \\ m_{10} & m_{11} & m_{12} \\ 0 & 0 & 1 \end{bmatrix} * \begin{bmatrix} X \\ Y \\ 1 \end{bmatrix} \quad (15)$$

where X' and Y' are the transformed coordinates of an image, X and Y are the original coordinates of the image, $m_{00}, m_{01}, m_{02}, m_{10}, m_{11}, m_{12}$ are the six coefficients of transformation. See [53] for the detailed information on the coefficient of transformation.

3) FACE VALIDATION

The Convolutional Neural Network (CNN) was used to train the face detection classifier. The input image was transformed into a 128-dimension vector. The Euclidean distances between the input image and the images in the database were computed to find the minimum distance, naming it the detected face. A confidence number output from the classifier indicated the probability of the AAQR enhanced image to be recognized as a human face. See (16) and [54] for details. A higher value corresponds to a higher confidence in the detection result.

$$Confidence = Softmax(I_{input}) \quad (16)$$

where I_{input} is the 128-dimension vector of a face image. In this paper, if the confidence is higher than 50%, the measured image will be considered as a correctly recognized human face. Additional details concerning this method appear in [50] and at https://github.com/TadasBaltrusaitis/OpenFace.

III. NIGHT IMAGES COLLECTION

To collect driver face images from nighttime driving, an experiment vehicle was used to drive on urban roads for data collection. A mobile phone was mounted on the windshield to capture driver face images at night. The resolution of the collected images was 640×480. See Fig. 3 for the experiment vehicle and the mounting position of the mobile phone for images collection. To categorize the collected images into three illumination groups (Up-Down, Left-Right, and Mixed), three coders with extensive experience in the subjective evaluation of images were recruited. If the illumination on a driver face was clearly separated into two parts, the image would be categorized into the Up-Down or the Left-Right group according to the coders' experience. Otherwise, the image would be binned to the Mixed illumination group. The illumination distribution in each image was subjectively assessed by two coders and mediated by a third, and then the image was binned to one of the illumination groups accordingly. Similar manual coding methods were used in naturalistic driving studies for ground truth labeling [55], [56]. In total, 900 images were extracted from the video with 300 images in each illumination group. See Fig. 4 for an illustration of the collected driver face images at night in each group.

FIGURE 3. Experimental vehicle.

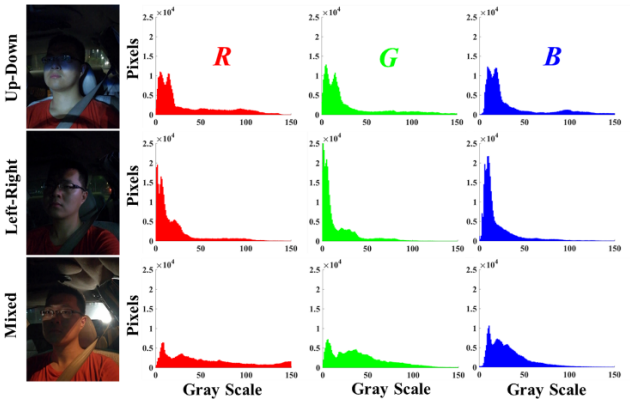

Illumination group	Number of images		Resolution
	Group number	Total	
Up-Down	300	900	640x480
Left-Right	300		
Mixed	300		

FIGURE 4. An illustration of the collected driver face images at night.

IV. ENHANCEMENT DETAILS AND DETECTION RESULTS

A. FACE DETAILS ENHANCEMENT

Fig. 5 shows the face details enhancement results using the proposed AAQR method. The original image has low contrast and low luminosity, hence, driver faces are difficult to be distinguished from the background. After image enhancement, the AAQR image becomes brighter with a higher contrast level. See Fig. 6 for the enhanced details. All the source code used in this study can be found at: https://github.com/hmwc123/AAQR-master

B. DETECTION OF DRIVER FACES IN NIGHTTIME

Fig. 6 illustrates the driver face detection results for each illumination category based on the proposed AAQR image enhancement method.

Table 3 presents the mean detection rate and the confidence for driver faces under different illumination conditions. For all the three illumination conditions, the original driver faces are essentially not detected. The correct detection rates based on AAQR images are 82%, 84% and 91% for the Up-Down, Left-Right, and Mixed illumination groups, respectively. The confidence values are 73%, 71% and 77%, respectively. Thus, the proposed AAQR method vastly improves the detection rates and confidences for driver faces at night for all the

FIGURE 5. Face details enhancement.

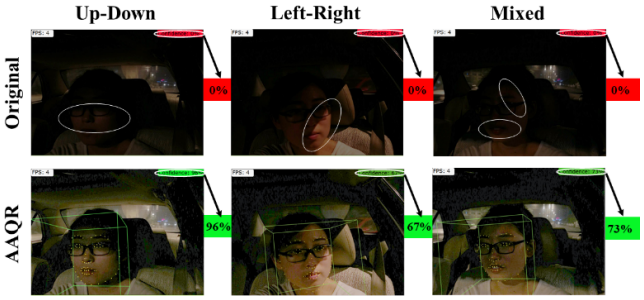

FIGURE 6. Detection of driver faces in nighttime (the percentage number indicates the detection confidence value).

TABLE 3. Correct detection rates for different nighttime illumination groups.

Illumination group	Original	Confidence	AAQR	Confidence
Up-Down	0%	0%	82%	73%
Left-Right	0%	0%	84%	71%
Mixed	4%	48%	91%	77%

three illumination patterns with the best outcome for the Mixed illumination.

C. COMPUTING TIME OF THE PROPOSED METHOD

Consistent with [57], for each original image, a photo editing tool was used to produce images with resolutions of 320×240, 1280×960 and 1920×1080. Derived from the same image, the produced images with different resolutions were more comparable with each other on the computing time. All experiments were running in MATLAB on a PC with a 3.3 GHz Intel I3-3220 Processor.

Using the proposed method in this study, the computing times for images with different resolutions are presented in Table 4. Results show that the mean computing time increases non-linearly with the increase of image resolution, which needs to be considered in online applications. The computing time is 0.25 s on average for a 640×480 image.

TABLE 4. Computing times for images with different resolutions.

Image Resolution	Computing time per image	Frames per second
320×240	0.06 s	16.0
640×480	0.25 s	4.0
1280×960	1.86 s	0.5
1920×1080	5.24 s	0.4

See the real-time performance on a video with dynamically changing light at https://youtu.be/LCddhLH9tZo.

V. DISCUSSION

To demonstrate the effectiveness of the proposed method, several state-of-the-art methods were employed to compare their performance with AAQR. The employed methods include SRIE, NPE, DONG, LIME, MF, and MSRCR. The driver faces recognition rate, confidence, Visual Information Fidelity (VIF) [59] and computing time of these methods were presented in this section. As a visual information fidelity criterion for full-reference image quality assessment, VIF was designed for and tested on degraded images. It is suitable for evaluating nonlinear image enhancement algorithms [59]. A higher VIF score means that the examined image is more likely to be correctly retained with the original image information.

Table 5 shows the comparison of detection rates, confidences and VIF scores for each algorithm and each illumination group. As presented, SRIE outperforms the others on most of the examined indexes except the detection rate of the Mixed and the Left-Right. AAQR ranks the second with the best detection rate in both the Mixed and the Left-Right.

Fig. 7 illustrates the enhancement results of driver face images at night using different algorithms. Results show that although the brightness is lower, the color of the enhanced images using SRIE is more natural with less noise. The results of NPE and MSRCR show apparent noise in the dark areas and detail loss in the bright areas. Similar undesired results are found in the enhanced images using DONG, LIME and MF. Although AAQR enhanced images is not as good as desired, the indexes shown in Table 5 prove that AAQR is a promising candidate to enhance nighttime images for driver face detection. This is because AAQR has an adaptive attenuation process which can reduce the interference of noise and prevent excessive loss of image information.

Interestingly, the detection rate of AAQR for the Mixed group ranks the highest among the three illumination groups. The histogram of the original face images shows that the histogram of each color channel is relatively smooth in the Mixed illumination group (See Fig. 4). Therefore, the attenuation limit distance is short, and most of the image information in the attenuation area belongs to noise. However, the histograms of each color channel for the Up-Down and Left-Right images are more concentrated in the edge regions. Therefore, the very low-light input hides intensive noise and

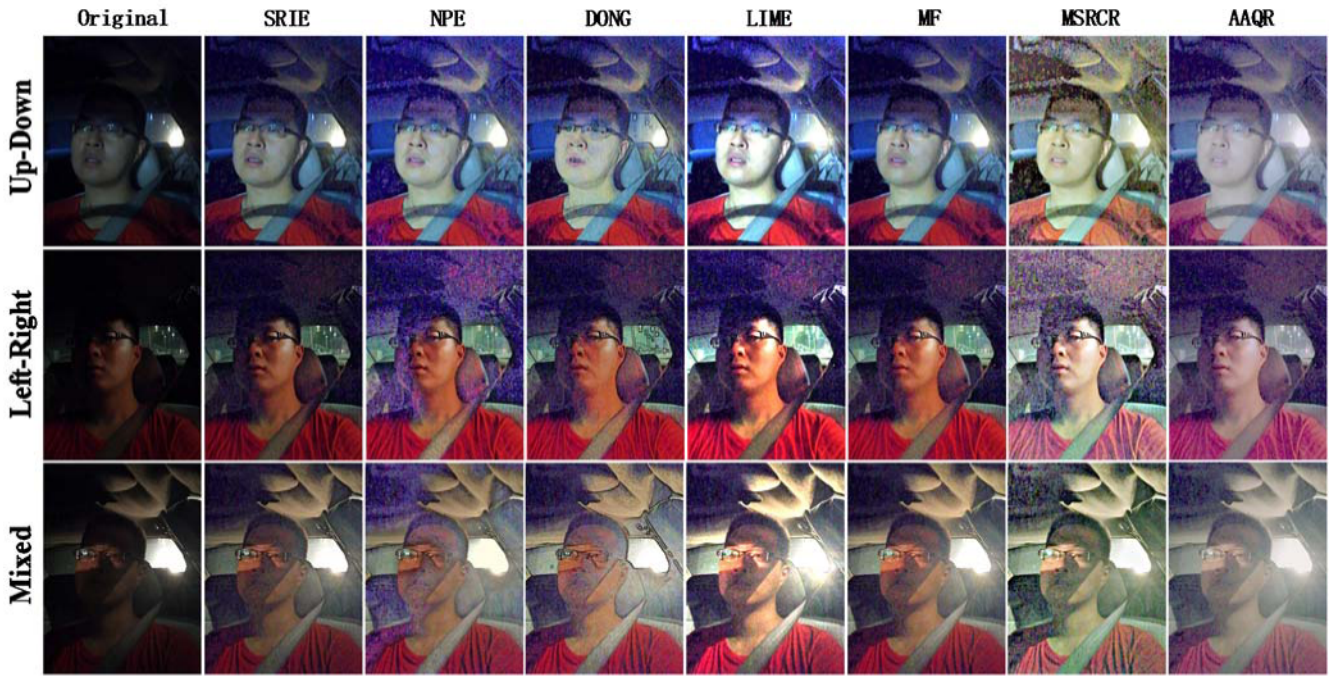

FIGURE 7. Enhancement results of driver face images at night using different algorithms.

TABLE 5. Comparison among different algorithms with three illumination group.

Illumination group	Examined indexes	SRIE	NPE	DONG	LIME	MF	MSRCR	AAQR
Up-Down	Recognition rate	**91%**	68%	71%	46%	80%	73%	82%
	Confidence	**78%**	66%	61%	56%	65%	67%	73%
	VIF	**0.3022**	0.1822	0.1774	0.1849	0.1967	0.1785	0.1924
Left-Right	Recognition rate	77%	78%	58%	71%	61%	74.7%	**84%**
	Confidence	**71%**	68%	61%	56%	51%	61%	71%
	VIF	**0.2942**	0.1814	0.1818	0.1518	0.1754	0.1652	0.1818
Mixed	Recognition rate	84%	74%	67%	82%	73%	80%	**91%**
	Confidence	**80%**	76%	69%	72%	67%	62%	77%
	VIF	**0.3104**	0.1789	0.1845	0.1786	0.2023	0.2135	0.2812

some useful image information. An attenuation limit distance may easily divide the useful image information into the attenuation area during the attenuation prediction process. Therefore, the processed images from the Up-Down and the Left-Right groups will lose more details than the Mixed illumination group and get lower detection rates.

The computing time needed for image processing is also an important evaluation factor indicating the online performance of an algorithm. The comparison of the computing time of different methods is shown in Table 6. The image resolution used for comparison is 640×480. The numbers in Table 6 show that although SRIE outperforms the other algorithms in terms of detection rates, it is too time-consuming to be applied in real-time applications. AAQR is faster than the other algorithms except for LIME. Thus, Comprehensively considering the recognition rate together with the computing time, AAQR achieves a better performance than the other algorithms.

TABLE 6. Comparison of computing times between different algorithms for a single 640×480 image.

Algorithm	Computing time per image	Frames per second
SRIE	11.1 s	0.1
NPE	11.9 s	0.1
DONG	0.36 s	2.8
LIME	0.21 s	4.7
MF	0.35 s	2.9
MSRCR	0.33 s	3.0
AAQR	0.25 s	4.0

One of the practical implications of the proposed method in automotive or transportation engineering is illustrated in Fig. 8. This proposed application scheme mainly focuses on online driver state monitoring and driver assistance strategies by context-aware music recommendation.

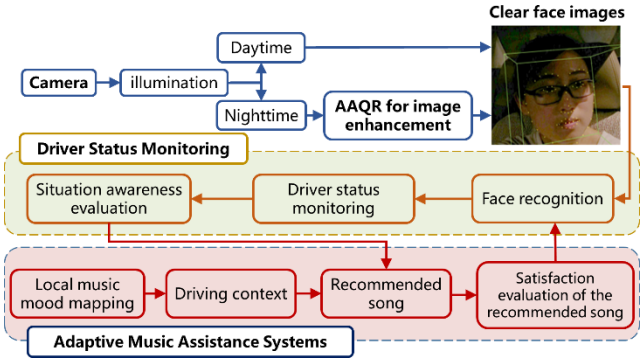

FIGURE 8. A practical application scheme of the proposed method in driver state monitoring.

Images collected by the camera would be recognized as daytime or nighttime images according to their illuminations. Usually, daytime is roughly defined from 6 am to 6 pm and nighttime from 6 pm to 6 am. Nighttime face images could be enhanced by the proposed AAQR method. Face detection and tracking algorithms could be developed to monitor driver state (e.g., fatigue) [58]. Based on the monitoring status, drivers' situation awareness level could be evaluated to determine if the driver needs assistance strategies. If needed, an appropriate song could be selected for recommendation according to the driving context and the mapping moods of the songs in the database. A song with appropriate music mood has been demonstrated to improve driving performance and drivers' delayed physiological reactions effectively [60]. Similar implications could be considered in other Advanced Driver Assistance Systems (ADASs) or human-vehicle cooperative driving strategies in autonomous driving systems [61].

The limitation of this study lies in the robustness of the proposed method in the Up-Down and Left-Right illumination conditions. As the histograms of the color channels for the Up-Down and Left-Right images are more concentrated in the edge regions, the attenuation distance in the proposed method would easily remove useful information from the images. Loss of useful image details deteriorates the face detection performance. Future work should focus on the following aspects: (1) Image details enhancement in the Up-Down and Left-Right illumination conditions needs to be further improved. (2) Near-infrared illumination systems and Retinex-based methods are the most primary solutions in Mixed lighting environment in nighttime. If these two methods could be fused together to compensate each other, it may significantly improve the driver face detection performance at night. (3) The nighttime image database of driver faces needs to be enriched.

VI. CONCLUSION

This paper proposes an Adaptive Attenuation Quantification Retinex (AAQR) method to enhance details in nighttime images for driver face detection tasks. Based on the enhanced images, a face detection method was used to evaluate the performance of the proposed AAQR method. Results showed that the overall detection rate of the nighttime images with different illuminance levels was 86%, which was 2-36% greater than the state-of-the-art algorithms. The performance of the AAQR method was better for the Mixed night illuminated situations rather than the Up-Down and the Left-Right distributed illumination situations. The narrower attenuation range effectively protected the quality of an image from losing the discriminative details. The mean computing time for a single 640×480 nighttime image using AAQR was less than most of the compared advanced methods, satisfactorily balancing between the detection rate and the computing time requirement for online driver state monitoring. These efforts significantly extend previous research to makes it possible for visible light cameras to detect driver states at night. The work presented in this paper provides a novel perspective for the promising deployment of nighttime driver assistance strategies in future Advanced Driver Assistance Systems (ADASs) or human-vehicle cooperative driving systems for autonomous vehicles.

ACKNOWLEDGMNET

(Jianhao Shen and Guofa Li contributed equally to this work.)

REFERENCES

[1] "Traffic safety facts," NHTSA, Washington, DC, USA, Tech. Rep. DOT HS 812 219, 2015.
[2] J. C. Stutts, J. W. Wilkins, J. S. Osberg, and B. V. Vaughn, "Driver risk factors for sleep-related crashes," *Accident Anal. Prevention*, vol. 35, no. 3, pp. 321–331, 2003.
[3] M.-H. Sigari, M.-R. Pourshahabi, M. Soryani, and M. Fathy, "A review on driver face monitoring systems for fatigue and distraction detection," *Int. J. Adv. Sci. Technol.*, vol. 64, pp. 73–100, Mar. 2014.
[4] J. Jo, S. J. Lee, K. R. Park, I.-J. Kim, and J. Kim, "Detecting driver drowsiness using feature-level fusion and user-specific classification," *Expert Syst. Appl.*, vol. 41, no. 4, pp. 1139–1152, Mar. 2014.
[5] P. M. Forsman, B. J. Vila, R. A. Short, C. G. Mott, and H. P. van Dongen, "Efficient driver drowsiness detection at moderate levels of drowsiness," *Accident Anal. Prevention*, vol. 50, no. 1, pp. 341–350, 2013.
[6] Z. Li, S. E. Li, R. Li, B. Cheng, and J. Shi, "Online detection of driver fatigue using steering wheel angles for real driving conditions," *Sensors*, vol. 17, no. 3, p. 495, 2017.
[7] C. Zhang, H. Wang, and R. Fu, "Automated detection of driver fatigue based on entropy and complexity measures," *IEEE Trans. Intell. Transp. Syst.*, vol. 15, no. 1, pp. 168–177, Feb. 2014.
[8] R. Fu, H. Wang, and W. Zhao, "Dynamic driver fatigue detection using hidden Markov model in real driving condition," *Expert Syst. Appl.*, vol. 63, pp. 397–411, Nov. 2016.
[9] J. Hu, "Automated detection of driver fatigue based on adaboost classifier with EEG signals," *Frontiers Comput. Neurosci.*, vol. 11, p. 72, Aug. 2017.
[10] S. G. Kong, J. Heo, B. R. Abidi, J. Paik, and M. A. Abidi, "Recent advances in visual and infrared face recognition—A review," *Comput. Vis. Image Understand.*, vol. 97, no. 1, pp. 103–135, 2005.
[11] B. Mandal, L. Li, G. S. Wang, and J. Lin, "Towards detection of bus driver fatigue based on robust visual analysis of eye state," *IEEE Trans. Intell. Transp. Syst.*, vol. 18, no. 3, pp. 545–557, Mar. 2017.
[12] D. Kang, H. Han, A. K. Jain, and S.-W. Lee, "Nighttime face recognition at large standoff: Cross-distance and cross-spectral matching," *Pattern Recognit.*, vol. 47, no. 12, pp. 3750–3766, 2014.
[13] M. Rezaei and R. Klette, "Vision-based driver-assistance systems," in *Computer Vision for Driver Assistance*. Cham, Switzerland: Springer, 2017, pp. 1–18.
[14] Y. Dong, Z. Hu, K. Uchimura, and N. Murayama, "Driver inattention monitoring system for intelligent vehicles: A review," *IEEE Trans. Intell. Transp. Syst.*, vol. 12, no. 2, pp. 596–614, Jun. 2011.

[15] A. J. Filtness, K. A. Armstrong, A. Watson, and S. S. Smith, "Sleep-related crash characteristics: Implications for applying a fatigue definition to crash reports," *Accident Anal. Prevention*, vol. 99, pp. 440–444, Feb. 2017.

[16] J. C. Chien, Y. S. Chen, and J. D. Lee, "Improving night time driving safety using vision-based classification techniques," *Sensors*, vol. 17, no. 10, p. 2199, 2017.

[17] M. J. Flores, J. M. Armingol, and A. de la Escalera, "Real-time warning system for driver drowsiness detection using visual information," *J. Intell. Robot. Syst.*, vol. 59, no. 2, pp. 103–125, 2010.

[18] J. Kang, D. V. Anderson, and M. H. Hayes, "Face recognition in vehicles with near infrared frame differencing," in *Proc. IEEE SP/SPE*, Aug. 2015, pp. 358–363.

[19] Q. Ji, Z. Zhu, and P. Lan, "Real-time nonintrusive monitoring and prediction of driver fatigue," *IEEE Trans. Veh. Technol.*, vol. 53, no. 4, pp. 1052–1068, Jul. 2004.

[20] B. Cyganek and S. Gruszczyński, "Hybrid computer vision system for drivers' eye recognition and fatigue monitoring," *Neurocomputing*, vol. 126, pp. 78–94, Feb. 2014.

[21] A. Dasgupta, A. George, S. L. Happy, and A. Routray, "A vision-based system for monitoring the loss of attention in automotive drivers," *IEEE Trans. Intell. Transp. Syst.*, vol. 14, no. 4, pp. 1825–1838, Dec. 2013.

[22] D. W. Hansen and Q. Ji, "In the eye of the beholder: A survey of models for eyes and gaze," *IEEE Trans. Pattern Anal. Mach. Intell.*, vol. 32, no. 3, pp. 478–500, Mar. 2010.

[23] L. M. Bergasa, J. Nuevo, M. A. Sotelo, R. Barea, and M. E. Lopez, "Real-time system for monitoring driver vigilance," *IEEE Trans. Intell. Transp. Syst.*, vol. 7, no. 1, pp. 63–77, Mar. 2006.

[24] F. Vicente, Z. Huang, X. Xiong, F. D. L. Torre, W. Zhang, and D. Levi, "Driver gaze tracking and eyes off the road detection system," *IEEE Trans. Intell. Transp. Syst.*, vol. 16, no. 4, pp. 2014–2027, Aug. 2015.

[25] E. H. Land and J. J. McCann, "Lightness and Retinex theory," *J. Opt. Soc. Amer.*, vol. 61, no. 1, pp. 1–11, 1971.

[26] M. Lecca, A. Rizzi, and R. P. Serapioni, "GRASS: A gradient-based random sampling scheme for Milano Retinex," *IEEE Trans. Image Process.*, vol. 26, no. 6, pp. 2767–2780, Jun. 2017.

[27] D. J. Jobson, Z.-U. Rahman, and G. A. Woodell, "A multiscale Retinex for bridging the gap between color images and the human observation of scenes," *IEEE Trans. Image Process.*, vol. 6, no. 7, pp. 965–976, Jul. 1997.

[28] K. Y. Shin, Y. H. Park, D. T. Nguyen, and K. R. Park, "Finger-vein image enhancement using a fuzzy-based fusion method with Gabor and retinex filtering," *Sensors*, vol. 14, no. 2, pp. 3095–3129, Feb. 2014.

[29] Z. Shi, M. Zhu, B. Guo, and M. Zhao, "A photographic negative imaging inspired method for low illumination night-time image enhancement," *Multimedia Tools Appl.*, vol. 76, no. 13, pp. 15027–15048, Jul. 2017.

[30] D. Zosso, G. Tran, and S. J. Osher, "Non-local Retinex—A unifying framework and beyond," *SIAM J. Imag. Sci.*, vol. 8, no. 2, pp. 787–826, 2015.

[31] Z. Rahman, D. J. Jobson, and G. A. Woodell, "Investigating the relationship between image enhancement and image compression in the context of the multi-scale retinex," *J. Vis. Commun. Image Represent.*, vol. 22, no. 3, pp. 237–250, 2011.

[32] B. Jiang, G. A. Woodell, and D. J. Jobson, "Novel multi-scale retinex with color restoration on graphics processing unit," *J. Real-Time Image Process.*, vol. 10, no. 2, pp. 239–253, 2015.

[33] H. Kuang, L. Chen, F. Gu, J. Chen, L. Chan, and H. Yan, "Combining region-of-interest extraction and image enhancement for nighttime vehicle detection," *IEEE Intell. Syst.*, vol. 31, no. 3, pp. 57–65, May 2016.

[34] S. Wang, J. Zheng, H.-M. Hu, and B. Li, "Naturalness preserved enhancement algorithm for non-uniform illumination images," *IEEE Trans. Image Process.*, vol. 22, no. 9, pp. 3538–3548, Sep. 2013.

[35] X. Fu, D. Zeng, Y. Huang, Y. Liao, X. Ding, and J. Paisley, "A fusion-based enhancing method for weakly illuminated images," *Signal Process.*, vol. 129, pp. 82–96, Dec. 2016.

[36] X. Fu, D. Zeng, Y. Huang, X.-P. Zhang, and X. Ding, "A weighted variational model for simultaneous reflectance and illumination estimation," in *Proc. IEEE CVPR*, Jun. 2016, pp. 2782–2790.

[37] X. Guo, Y. Li, and H. Ling, "LIME: Low-light image enhancement via illumination map estimation," *IEEE Trans. Image Process.*, vol. 26, no. 2, pp. 982–993, Feb. 2017.

[38] X. Dong *et al.*, "Fast efficient algorithm for enhancement of low lighting video," in *Proc. IEEE ICME*, Jul. 2011, pp. 1–6.

[39] B.-H. Chen, Y.-L. Wu, and L.-F. Shi, "A fast image contrast enhancement algorithm using entropy-preserving mapping prior," *IEEE Trans. Circuits Syst. Video Technol.*, to be published, doi: 10.1109/TCSVT.2017.2773461.

[40] Y.-H. Shiau, P.-Y. Chen, H.-Y. Yang, and S.-Y. Li, "A low-cost hardware architecture for illumination adjustment in real-time applications," *IEEE Trans. Intell. Transp. Syst.*, vol. 16, no. 2, pp. 934–946, Apr. 2015.

[41] M. Versaci, F. C. Morabito, and G. Angiulli, "Adaptive image contrast enhancement by computing distances into a 4-dimensional fuzzy unit hypercube," *IEEE Access*, vol. 5, pp. 26922–26931, 2017.

[42] B. H. Chen, "An illuminance attenuation prior to contrast enhancement for vision-based advanced driver assistance systems," in *Proc. BDAW*, New York, NY, USA, 2016, p. 38.

[43] A. Jabeen, M. M. Riaz, N. Iltaf, and A. Ghafoor, "Image contrast enhancement using weighted transformation function," *IEEE Sensors J.*, vol. 16, no. 20, pp. 7534–7536, Oct. 2016.

[44] S. Guo, S. Pan, L. Shi, P. Guo, Y. He, and K. Tang, "Visual detection and tracking system for a spherical amphibious robot," *Sensors*, vol. 17, no. 4, p. 870, Apr. 2017.

[45] Y. Wang, H. Wang, C. Yin, and M. Dai, "Biologically inspired image enhancement based on Retinex," *Neurocomputing*, vol. 177, pp. 373–384, Feb. 2016.

[46] S. Park, S. Yu, B. Moon, S. Ko, and J. Paik, "Low-light image enhancement using variational optimization-based Retinex model," *IEEE Trans. Consum. Electron.*, vol. 63, no. 2, pp. 178–184, May 2017.

[47] H. Lin and Z. Shi, "Multi-scale retinex improvement for nighttime image enhancement," *Optik—Int. J. Light Electron Opt.*, vol. 125, no. 24, pp. 7143–7148, Dec. 2014.

[48] Z. Rahman, D. J. Jobson, and G. A. Woodell, "Multi-scale retinex for color image enhancement," in *Proc. IEEE ICIP*, Sep. 1996, pp. 1003–1006.

[49] M. G. Kang and A. K. Katsaggelos, "Simultaneous iterative image restoration and evaluation of the regularization parameter," *IEEE Trans. Signal Process.*, vol. 40, no. 9, pp. 2329–2334, Sep. 1992.

[50] T. Baltrušaitis, P. Robinson, and L.-P. Morency, "OpenFace: An open source facial behavior analysis toolkit," in *Proc. IEEE WACV*, Mar. 2016, pp. 1–10.

[51] J. Wright, A. Y. Yang, A. Ganesh, S. S. Sastry, and Y. Ma, "Robust face recognition via sparse representation," *IEEE Trans. Pattern Anal. Mach. Intell.*, vol. 31, no. 2, pp. 210–227, Feb. 2009.

[52] P. F. Felzenszwalb, R. B. Girshick, D. McAllester, and D. Ramanan, "Object detection with discriminatively trained part-based models," *IEEE Trans. Pattern Anal. Mach. Intell.*, vol. 32, no. 9, pp. 1627–1645, Sep. 2010.

[53] V. Kazemi and J. Sullivan, "One millisecond face alignment with an ensemble of regression trees," in *Proc. IEEE CVPR*, Jun. 2014, pp. 1867–1874.

[54] F. Schroff, D. Kalenichenko, and J. Philbin, "FaceNet: A unified embedding for face recognition and clustering," in *Proc. IEEE CVPR*, Jun. 2015, pp. 815–823.

[55] L. Fridman, P. Langhans, J. Lee, and B. Reimer, "Driver gaze region estimation without use of eye movement," *IEEE Intell. Syst.*, vol. 31, no. 3, pp. 49–56, May 2016.

[56] K. D. Kusano, R. Chen, J. Montgomery, and H. C. Gabler, "Population distributions of time to collision at brake application during car following from naturalistic driving data," *J. Saf. Res.*, vol. 54, pp. 95–104, Sep. 2015.

[57] K.-Y. Park and S.-Y. Hwang, "An improved Haar-like feature for efficient object detection," *Pattern Recognit. Lett.*, vol. 42, pp. 148–153, Jun. 2014.

[58] C. Zhao, Y. Zhang, X. Zhang, and J. He, "Recognition of driver's fatigue expression using local multiresolution derivative pattern," *J. Intell. Fuzzy Syst.*, vol. 30, no. 1, pp. 547–560, 2016.

[59] H. R. Sheikh and A. C. Bovik, "Image information and visual quality," *IEEE Trans. Image Process.*, vol. 15, no. 2, pp. 430–444, Feb. 2006.

[60] X. Hu *et al.*, "SAfeDJ: A crowd-cloud codesign approach to situation-aware music delivery for drivers," *ACM Trans. Multimedia Comput., Commun. Appl.*, vol. 12, no. 1s, pp. 1–24, Oct. 2015.

[61] G. Li, S. E. Li, and B. Cheng, "Field operational test of advanced driver assistance systems in typical chinese road conditions: The influence of driver gender, age and aggression," *Int. J. Automot. Technol.*, vol. 16, no. 5, pp. 739–750, 2015.

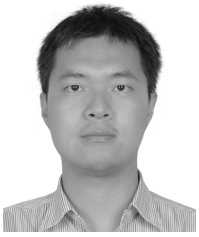

JIANHAO SHEN received the B.S. degree in mechanical engineering from Chongqing Three Gorges University, Chongqing, China, in 2013. He is currently pursuing the Ph.D. degree with the College of Mechatronics and Control Engineering, Shenzhen University, Shenzhen, China. His main research interests include facial expression recognition, image enhancement, and driver fatigue detection systems development.

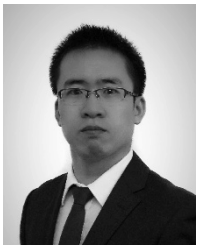

GUOFA LI received the Ph.D. degree from Tsinghua University, Beijing, China, in 2016. From 2012 to 2013, he was a Visiting Scholar with the University of Michigan Transportation Research Institute. He is currently an Assistant Professor with the College of Mechatronics and Control Engineering, Shenzhen University, Guangdong, China. His research interests include autonomous vehicles, driver behavior, advanced driver assistance systems, machine learning techniques, and human factors in automotive and transportation engineering. He was a recipient of the NSK Sino-Japan Outstanding Paper Prize from NSK Ltd. in 2014 and the Excellent Young Engineer Innovation Award from SAE-China in 2017.

WEIQUAN YAN is currently pursuing the B.S. degree with the College of Mechatronics and Control Engineering, Shenzhen University, Shenzhen, China. His main research interests include driver behavior modeling and advanced driver assistance systems development.

WENJIN TAO received the bachelor's and master's degrees from the Beijing Institute of Technology, Beijing, China. He is currently pursuing the Ph.D. degree with the Department of Mechanical and Aerospace Engineering, Missouri University of Science and Technology, Rolla, MO, USA.

His research interests include smart manufacturing, human activity recognition, deep learning, and digital design.

GANG XU received the B.S. degree in control engineering from Beihang University, Beijing, China, in 1982, and the Ph.D. degree in engine-control engineering from the Nanjing University of Aeronautics and Astronautics, Nanjing, China, in 1995. From 1987 to 1989, he was a Visiting Research Fellow with Louisiana State University, Baton Rouge, LA, USA.

From 1996 to 1997, he held a post-doctoral position at Sussex University, Brighton, U.K. Since 1998, he has been a Professor with the College of Mechatronics and Control Engineering, Shenzhen University, Shenzhen, China. His research interests include aeroengines, electric vehicles, and traffic engineering.

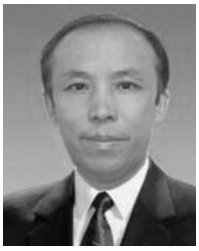

DONGFENG DIAO received the Ph.D. degree from Tohoku University, Japan, in 1992. He was a Research Associate with Tohoku University from 1993 to 1994 and an Associate Professor with Shizuoka University, Japan, from 1995 to 2002. In 1996, he was invited to The Ohio State University as a JSPS Research Fellow.

His current research interests include nanosurface science and engineering with an emphasis on mechanical science, FEM-MD contact mechanics, ECR plasma physics, AFM biomechanics, and nanotribology.

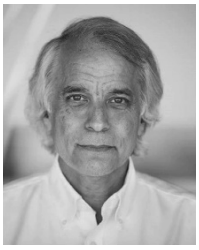

PAUL GREEN received the M.S. and Ph.D. degrees from the University of Michigan, Ann Arbor, MI, USA, in 1974 and 1979, respectively. He is currently a Research Professor with the Driver Interface Group, University of Michigan Transportation Research Institute, Ann Arbor, MI, USA, and an Adjunct Professor with the Department of Industrial and Operations Engineering, University of Michigan. He teaches automotive human factors and human–computer interaction classes. He is also the Leader of the University's Human Factors Engineering Short Course, the flagship continuing education course in the profession, currently in its 59th year. His research interests include driver interfaces and driver workload, and the development of standards to get research into practice. He is a past President of the Human Factors and Ergonomics Society.